Noninvasive Quantification of Jeopardized Myocardial Mass in Dogs Using 2-Dimensional Echocardiography and Thallium-201 Tomography

ROBERT J. WEISS, MD, ANDREW J. BUDA, MD, STANISLAW PASYK, MD, WILLIAM W. O'NEILL, MD, JOHN W. KEYES, Jr., MD, and BERTRAM PITT, MD

The evaluation of jeopardized myocardial mass is important in defining the effect of interventions during myocardial infarction. To quantitate the in vivo mass at risk, 2-dimensional echocardiography (2-D echo) and thallium-201 single-photon emission computed tomography (SPECT) was performed in 10 closed-chest dogs after circumflex coronary artery occlusion. The 2-D images were manually digitized to compute left ventricular (LV) mass using a modified Simpson's rule algorithm. This measure of LV mass correlated well with the actual LV mass (r = 0.97). Perfused myocardial mass was estimated from thallium SPECT images 4 hours after occlusion using a region-growing algorithm. After the dogs were killed, the jeopardized mass was outlined using a dual perfusion staining technique using triphenyltetrazolium chloride and Evans blue dye. The actual perfused mass was well estimated by the thallium images (r = 0.96). The noninvasively determined mass at risk was calculated as: 2-D mass − thallium SPECT mass, and correlated well with the pathologically determined mass at risk (r = 0.91). Thus, the jeopardized mass may be determined noninvasively by using 2-D echo and thallium-201 tomography. This approach may provide further information regarding the effect of intervention therapy on jeopardized myocardium.

(Am J Cardiol 1983;52:1340–1344)

The evaluation of recent attempts to limit the size of acute myocardial infarction in patients is limited by the inability to define accurately the size of the ultimate infarction in terms of the initial area of jeopardized, or "at risk," myocardium. Attempts have been made to size infarctions using ST-segment mapping,[1] planar thallium-201 imaging,[2] computed axial tomography,[3] body surface potential mapping,[4] 2-dimensional echocardiography (2-D echo),[5,6] creatine kinase-MB activity,[7] and radionuclide scanning[8] in order to study prognosis[9,10] and protective effects of various interventions. However, none of these techniques defines, in a given experimental animal or patient, the area of potential infarction. This area at risk has been defined in terms of the size of the perfusion bed of the occluded artery.[11–15] Although the amount of ultimate necrosis and the size of the occluded perfusion bed are related, there is great variability even when the coronary artery occlusion is experimentally placed at identical anatomic sites.[11,12] The present study uses 2-D echo and thallium-201 (Tl-201) single-photon emission computed tomography (SPECT) to develop a noninvasive method of defining the area of myocardium at risk of necrosis early, after a myocardial infarction.

From the Divisions of Cardiology and Nuclear Medicine, University of Michigan Medical Center, Ann Arbor, Michigan. This study was supported in part by a Grant-in-Aid from the American Heart Association of Michigan, Lathrup Village, Michigan and Grant HL 21707 from the National Heart, Lung, and Blood Institute, National Institutes of Health, Bethesda, Maryland. Manuscript received May 16, 1983; revised manuscript received August 24, 1983, accepted August 30, 1983.

Address for reprints: Andrew J. Buda, MD, Division of Cardiology, University of Michigan Medical Center, 1405 East Ann Street, Ann Arbor, Michigan 48109.

Methods

Surgical preparation: Eleven dogs were anesthetized with morphine and sodium pentobarbital and placed on a respirator. Under aseptic conditions, a left thoracotomy was performed, and a mercury-filled cuff occluder, which was controlled externally by a piston screw device, was implanted on the left circumflex coronary artery (LCCA). The chest was closed and the pneumothorax evacuated. The dogs were allowed to recover from the surgery for 14 days. Constriction of the LCCA was achieved in the conscious, sedated dog by a few turns of the screw-driven piston on the occluder. Total LCCA occlusion was estimated from the number of turns of the screw after precalibration before implantation.

Two-dimensional echocardiographic studies: The 2-D echoes were performed with the dogs in the right lateral decubitus position on a specially constructed table with a cutout

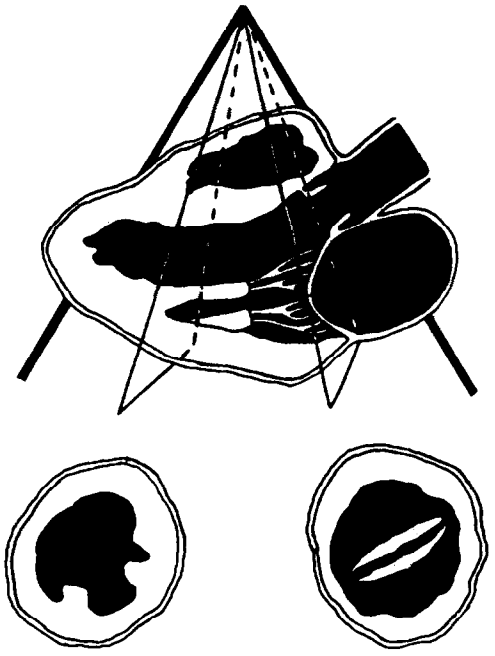

FIGURE 1. Two-dimensional echocardiographic image (schematic) in the long-axis view and 2 short-axis views (midpapillary muscle and mitral valve).

FIGURE 2. Representative end-diastolic frame of a 2-dimensional echocardiogram in the short axis at the midpapillary level.

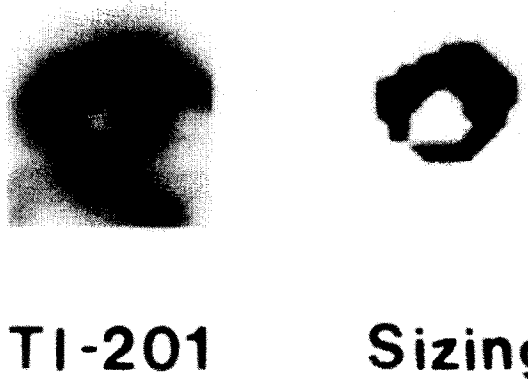

FIGURE 3. Tomographic thallium-201 (Tl-201) image (**left**) with computer-derived image using sizing program (**right**).

allowing positioning of the transducer. Images were obtained just before occlusion of the LCCA. Hard copies of end-diastolic and end-systolic freeze frames, timed to correspond to the onset of the QRS and end of the T wave, respectively, were generated in the short axis at the midpapillary muscle and the mitral valve levels, and in the long axis (Fig. 1 and 2). Using these freeze frames, the endocardial and epicardial borders were manually digitized, and the enscribed areas were determined and used to calculate volumes according to the formula of Folland et al[16]: $V = (A_m)L/3 + (A_m + A_p)/2\ L/3 + 1/3(A_p)L/3$, where V = volume, A_m = short-axis area at the mitral valve level, L = longest length in the long-axis view, and A_p = short-axis area at the papillary muscle level. The papillary muscles themselves were excluded. The endocardial volume was subtracted from the epicardial volume to give the volume of the myocardium. The myocardial volume was multiplied by the specific gravity of myocardial muscle (1.05) to determine myocardial mass.

Radionuclide imaging technique: The dogs were positioned within a rotating gamma camera tomograph. The detector was equipped with a high-resolution, low-energy, parallel-hole collimator and was positioned as close to the dog as possible. Two millicuries of Tl-201 were injected intravenously 4 hours after occlusion and imaging was begun 10 minutes later. Images were acquired every 5.8° of rotation, yielding 32 images. Each image was digitized into a 64 × 64 matrix and stored on magnetic disk in a small computer. Tomographic sections that encompassed the entire volume of the myocardium were then reconstructed using a filtered back projection algorithm without attenuation compensation.[17]

The reconstructed tomographic sections were displayed on a computer terminal. Using the computer display, the operator flagged an appropriate starting point within the perfused volume of myocardium. The program then traced out the total volume corresponding to the perfused myocardium on all tomographic sections (Fig. 3). The algorithm used was based on a region-growing technique that determines the border of the perfused zone based on threshold and rate-of-change criteria. This method was validated in phantom studies and found to be accurate over the range of 20 to 400 ml (Keyes JW, Jr., unpublished data). The total volume of the perfused region was then calculated by multiplying the volume of a single pixel (0.25 ml) by the total number of pixels within the computer-defined perfused volume. The volume determination was then multiplied by the specific gravity of myocardial muscle to obtain the perfused myocardial mass.

Pathologic quantification: The dogs were killed and the excised hearts were rinsed with saline, weighed and attached to a perfusion apparatus.[18] The coronary circulation was flushed by perfusing the aorta with 1 liter of warm saline. The LCCA was then cannulated at the point of the occlusion and perfused with warm, buffered (10 m*M* sodium phosphate, pH 7.4), triphenyltetrazolium chloride (TPT), while buffered 0.3% Evans blue dye was delivered, at an equal pressure (100 mm Hg), into the left anterior descending and right coronary artery through the aorta. Differential perfusion of the LCCA defined both the anatomic area at risk for infarction as well as the area of infarction. This was based on the ability of dehydrogenases present in viable myocardium to react with TPT.[19] With this dual injection technique, the myocardium not at risk was stained dark blue with the Evans blue. The boundaries of the area at risk were stained brick red with the TPT, and the area of infarction appeared yellow. After ap-

TABLE I Total Myocardial Mass as Determined by 2-Dimensional Echocardiography Versus Pathologically Determined Myocardial Mass

Dog	Echo Mass (g)	Actual Mass (g)
2	113	134
3	166	171
4	126	149
5	118	130
6	112	114
7	128	134
8	163	187
9	206	239
10	147	165
11	150	166

TABLE II Perfused Myocardial Mass as Determined by Thallium-201 Scintigraphy Versus Pathologically Determined Perfused Mass

Dog	Tl-201 Perfused Mass (g)	Actual Perfused (Viable) Mass (g)
2	82	80
3	147	134
4	62	60
5	89	84
6	90	82
7	87	80
8	98	105
9	149	143
10	102	107
11	98	108

Tl-201 = thallium-201.

proximately 15 minutes, the perfused hearts were transversely sliced into 1-cm-thick sections. Both sides of each section were then traced on an acetate transparency and divided into the 3 areas (viable, risk and infarcted). The average area for each myocardial ring was multiplied by the weight of each ring to give the mass of myocardium viable, at risk and infarcted.

Noninvasive calculation of area at risk: The total myocardial mass was obtained from the 2-D echocardiographic images. The mass of perfused myocardium (excluding infarcted and ischemic tissue) was obtained from the Tl-201 tomographic images. Risk mass was then obtained by subtracting the perfused mass from the total mass.

Statistical methods: Results are presented as the mean ± standard error of the mean. Correlation coefficients were determined by the least-squares method.

Results

Eleven dogs that weighed 31.0 ± 1.1 kg underwent surgery and chronic instrumentation. One dog fibrillated and died approximately 20 minutes after acute LCCA occlusion and was excluded from analysis. The LCCA occlusion was left in place for 4.7 ± 0.1 hours. The area at risk for infarction from the LCCA occlusion as determined by TPT staining was 37 ± 2% of the LV mass. The area of actual infarction was 11 ± 3% of the LV mass. The total LV mass as determined by the 2-D echocardiographic images showed an excellent correlation with the actual pathologic mass (r = 0.97; slope = 0.93; x intercept = −5.6) (Table I, Fig. 4). The 2-D echocardiographic images consistently slightly underestimated the true LV mass (mean error 14 ± 4%). The Tl-201 tomographic images also showed an excellent correlation with the pathologically determined viable perfused mass (r = 0.96; slope = 1.17; x intercept = 6.6) (Table II, Fig. 5), but tended to overestimate mass in 7 of 10 dogs (mean error 7 ± 1%).

The calculated risk mass was determined by subtracting the perfused mass as measured by Tl-201 from the total LV mass as measured by 2-D echo. Again, there was an excellent correlation with the actual risk mass

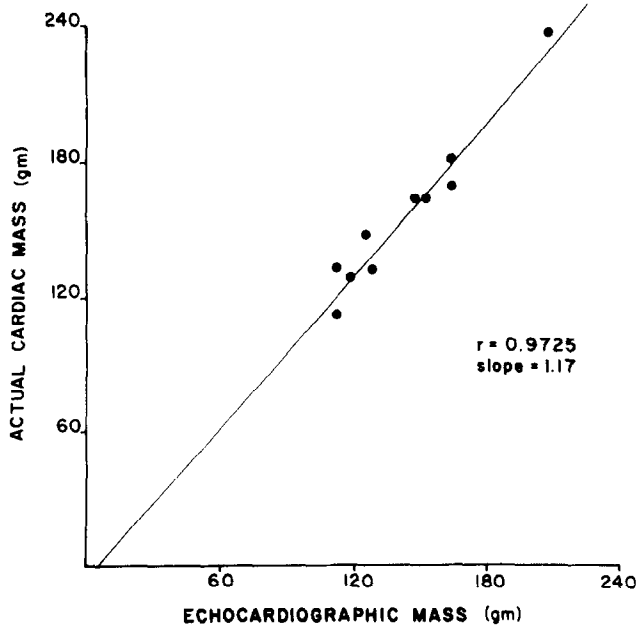

FIGURE 4. Correlation of 2-dimensional echocardiographic calculated total myocardial mass and pathologically determined total myocardial mass.

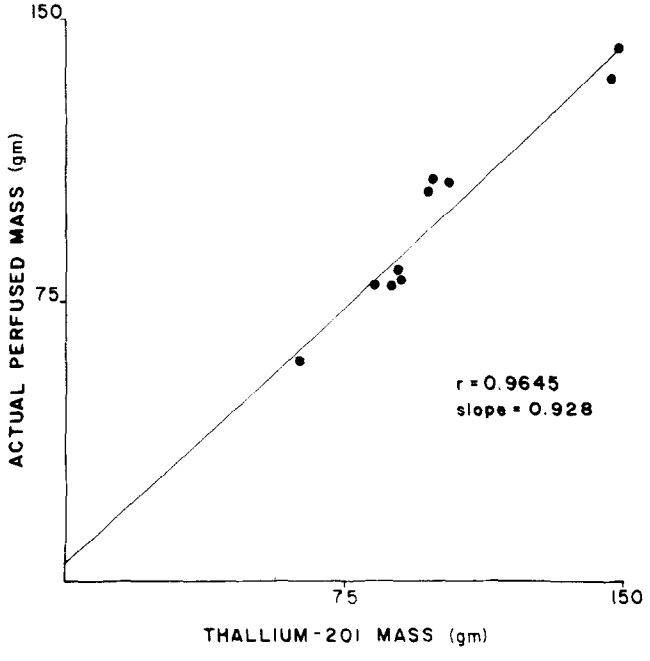

FIGURE 5. Correlation of thallium-201 single-photon emission computed tomography calculated by perfused mass and pathologically determined perfused mass.

TABLE III Calculated Risk Mass Versus Pathologically Determined Risk Mass

Dog	Calculated risk mass (g) (Functional)	Actual risk mass (g) (Anatomic)
2	30	55
3	19	37
4	64	89
5	29	46
6	21	32
7	41	54
8	66	82
9	58	96
10	45	59
11	52	57

as measured pathologically (r = 0.91; slope = 1.16; x intercept = 9.9) (Table III, Fig. 6). The calculated risk mass tended to underestimate pathologic risk mass (mean error 31 ± 4%).

Discussion

The area of jeopardized, or "at risk," myocardium has been defined as the area distal to a high grade coronary artery stenosis or occlusion.[13] Although the amount of necrosis parallels the area at risk, at least in dogs, there is great inherent variability in the exact relationship.[12] Even with experimental occlusions placed at the same anatomic site, there is wide variability in the extent of the ultimate infarction.[12] The variation in infarct size is related to a variation in the transmural extent of the infarction and has ranged from 50 to 88% of the perfused bed at risk.[13] Because of this inherent variability of infarct size, the effect of a therapeutic intervention may require a large number of animals for adequate assessment. This may be avoided by relating the infarct size to the size of the risk region,[12] which would improve the accuracy of intervention studies during acute myocardial infarction.

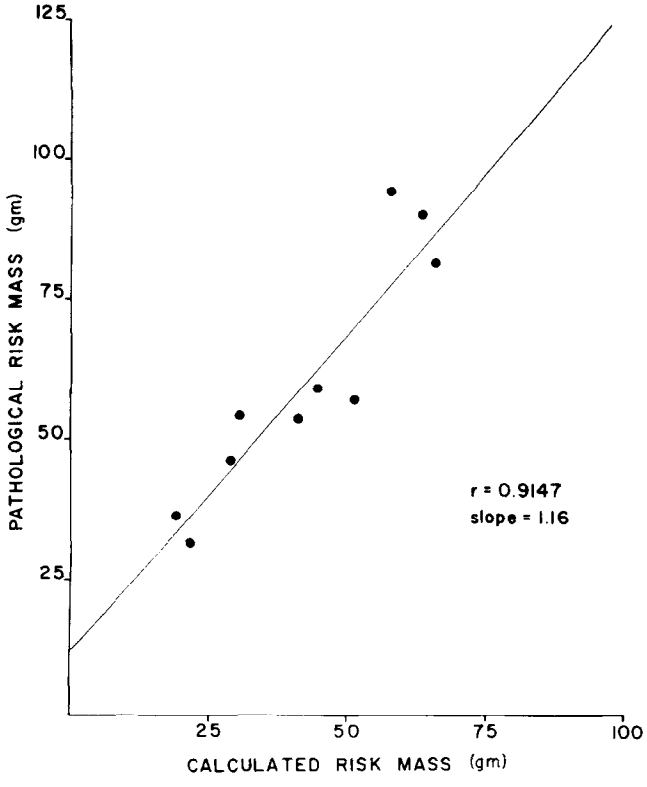

FIGURE 6. Correlation of calculated myocardial risk area and pathologically determined risk area.

Although a variety of techniques, primarily using dyes[11,12] or gels,[13,14] have been used to define jeopardized myocardium, it is important to distinguish between "functional" and "anatomic" myocardial area at risk. The functional myocardium at risk is usually defined using methods that take into account the contribution of collateral flow. The anatomic myocardium at risk is generally delineated using postmortem coronary injections, which tend to negate the influence of collaterals. Thus, the anatomic area at risk may not correspond to the functional risk area and may be expected to be larger than the latter if the effect of collateral flow is important. This is supported by recent work of Geary et al,[11] who used microvascular dye-injection techniques, which allowed accurate determination of the anatomic perfusion bed of an occluded artery and high resolution epicardial ST-segment mapping to assess the accuracy of the perfusion bed to represent the region at risk of infarction. Although the epicardial area of the anatomic perfusion bed correlated closely with the epicardial area of ST-segment mapping at 2 minutes after occlusion in the dog, by 30 minutes there was a progressive and variable reduction in ST-segment elevation reflecting gradual recruitment of existing collateral channels from adjacent perfusion beds. In dogs, collaterals between epicardial branches of coronary arteries are common and contribute to a variable but small collateral circulation. Thus, after abrupt occlusion, this initial level of collateral function may modify the risk zone and be an important determinant of the size of the infarction that results.[20]

Two-dimensional echocardiography has been used to directly determine infarct size,[5,6] but not to measure risk area. Although 2-D echocardiographic determination of infarct size demonstrates a good correlation with actual infarct size, the regional abnormalities seen tend to overestimate infarct size, probably because of a tethering phenomenon in adjacent nonischemic tissue.[6] The ability of 2-D echo to directly estimate risk zone was not addressed in our study, but similar tethering effects may make risk area quantification difficult. In the present study, total LV mass was determined from the 2-D echocardiographic images using the formula that Folland et al[16] validated in an isolated dog heart model. Although this formula still requires geometric assumptions, it does not require fixing a point of reference to measure wall motion. In our study, 2-D echo was highly accurate in estimating total LV mass (r = 0.97). It consistently caused a slight underestimation, perhaps partly because we did not include the papillary muscles in the analysis.

Thallium-201 imaging has also been used to estimate the size of a myocardial infarction. The recent introduction of SPECT imaging has improved the ability to define 3-dimensional detail of ischemic and infarcted myocardium and, as a result, has provided better

quantitative estimates of infarct extent.[17] In patients studied at 4 weeks after infarction, there was a poor relation between the planar Tl-201 image estimation of infarct size and the estimation of CK-MB (r = 0.69); this was greatly improved using SPECT (r = 0.89).[2] We have used SPECT in isolated dog hearts to calculate both viable mass (r = 0.87), infarcted mass (r = 0.90), and the percentage of the left ventricle infarcted (r = 0.87).[17] In both of these studies,[2,17] the infarcted mass was determined by developing computer-aided calculations of the size of the nonvisualized (thallium defect) region. This requires the assumption of uniformity of wall thickness and motion in the infarcted and noninfarcted regions. If the damaged tissue is thinned or dyskinetic, one cannot assume uniform thickness. In the present study, this work was extended to a closed-chest dog model and only the visualized (perfused) area on the thallium image was quantified. This eliminated any geometric assumptions and was based solely on the number of pixels occupied by the perfused left ventricle. In our study, SPECT was highly accurate (r = 0.96) in determining the mass of perfused tissue. The uptake of Tl-201 is known to correlate well with myocardial blood flow,[21] and this study extends this observation to tomographic images obtained in closed-chest dogs. The Tl-201 imaging overestimated the perfused mass in 7 of 10 dogs. This discrepancy might be explained by our dual perfusion staining method of anatomically defining the risk area which excluded collateral flow into the perfusion bed of the occluded vessel. Since the Tl-201 estimation of perfused mass may depend both on anatomic risk area and collateral flow within the risk area, the discrepancies we noted between in vivo and pathologic estimates of perfused, viable tissue may be a real phenomenon.

Thus, in the present study, 2-D echo was used to calculate total myocardial mass, and SPECT was used to calculate perfused myocardial mass. The subtraction of perfused mass from total mass gave an estimate of the mass of myocardium at risk. These analyses were validated by comparison with pathologically determined masses. The dual dye perfusion technique has been used[18,22,23] in defining in vitro risk, nonrisk and infarcted areas. The simultaneous perfusion under equal pressure of Evans blue and the TPT should eliminate the entrance of either dye into collateral channels and thus provide a measure of the anatomic rather than functional risk area. The difference between functional and anatomic risk area might help explain the consistent underestimation of the risk mass determined in our study in vivo by the combined 2-D echo-thallium SPECT technique compared to the in vitro pathologically determined risk mass. An additional or alternative explanation might be found in work that has shown an early increase in myocardial volume during the evolution of an infarction due to edema.[24] The tissue fluid has a lower density than that of myocardial tissue and would cause the conversion of Tl-201 perfused volume to mass to be artifactually elevated.

Acknowledgment: We gratefully acknowledge Mary Sue LeMire and Beth Harkness for their valuable technical assistance. We thank Benedict R. Lucchesi, PhD, MD, for his assistance with the dual staining perfusion technique. We also thank Sharon Haglund for preparing the manuscript.

References

1. **Essen RV, Merx W, Effert S.** Spontaneous course of ST-segment elevation in acute anterior myocardial infarction. Circulation 1979;59:105–112.
2. **Tamaki S, Nakajima H, Murakami T, Yui Y, Kambara H, Kadota K, Yoshida A, Kawai C, Tamaki N, Mukai T, Ishii Y, Torizuka K.** Estimation of infarct size by myocardial emission computed tomography with thallium-201 and its relation to creatine kinase-MB release after myocardial infarction in man. Circulation 1982;66:994–1001.
3. **Doherty PW, Lipton MJ, Berninger WH, Skioldebrand CG, Carlsson E, Redington RW.** Detection and quantification of myocardial infarction in vivo using transmission computed tomography. Circulation 1981;63:597–606.
4. **Mirvis DM.** Body surface distribution of repolarization potentials after a myocardial infarction. II. Relationship between isopotential mapping and ST-segment potential summation methods. Circulation 1981;63:623–631.
5. **Lieberman AN, Weiss JL, Jugdutt BI, Becker LC, Bulkley BH, Garrison JG, Hutchins GM, Kallman CA, Weisfeldt ML.** Two-dimensional echocardiography and infarct size: relationship of regional wall motion and thickening to the extent of myocardial infarction in the dog. Circulation 1981;63:739–746.
6. **Wyatt HL, Meerbaum S, Heng MK, Rit J, Gueret P, Corday E.** Experimental evaluation of the extent of myocardial dyssynergy and infarct size by two-dimensional echocardiography. Circulation 1981;63:607–614.
7. **Shell WE, Lavelle JF, Covell JW, Sobel BE.** Early estimation of myocardial damage in conscious dogs and patients with evolving acute myocardial infarction. J Clin Invest 1973;52:2579–2590.
8. **Morrison J, Coromilas J, Munsey D, Robbins M, Zema M, Chiaramida S, Reiser P, Scherr L.** Correlation of radionuclide estimates of myocardial infarction size and release of creatine kinase-MB in man. Circulation 1980;62:277–287.
9. **Page DL, Caulfield JB, Kastor JA, DeSanctis RW, Sanders CA.** Myocardial changes associated with cardiogenic shock. N Engl J Med 1971;285:133–137.
10. **Sobel BE, Bresnahan GF, Shell WE, Yoder RD.** Estimation of infarct size in man and its relationship to prognosis. Circulation 1972;46:640–648.
11. **Geary GG, Smith GT, McNamara JJ.** Defining the anatomic perfusion bed of an occluded coronary artery and the region at risk to infarction. Am J Cardiol 1981;47:1240–1247.
12. **Lowe JE, Reimer KA, Jennings RB.** Experimental infarct size as a function of the amount of myocardium at risk. Am J Pathol 1978;90:363–377.
13. **Lee JT, Ideker RE, Reimer KA.** Myocardial infarct size and location in relation to the coronary vascular bed at risk in man. Circulation 1982;64:526–534.
14. **Jugdutt BI, Hutchins GM, Bulkley BH, Becker LC.** Myocardial infarction in the conscious dog: three-dimensional mapping of infarct, collateral flow and region at risk. Circulation 1979;60:1141–1150.
15. **Becker LC, Schuster EH, Jugdutt BI, Hutchins GM, Bulkley BH.** Relationship between myocardial infarct size and occluded bed size in the dog: difference between left anterior descending and circumflex coronary artery occlusions. Circulation 1983;67:549–557.
16. **Folland ED, Parisi AF, Moynihan PF, Jones DR, Feldman CL, Tow DE.** Assessment of left ventricle ejection fraction and volume by real-time, two-dimensional echocardiography. Circulation 1979;60:760–766.
17. **Keyes JW Jr, Brady TJ, Leonard PF, Svetkoff DB, Winter SM, Rogers WL, Rose EA.** Calculation of viable and infarcted myocardial mass from thallium-201 tomograms. J Nucl Med 1981;22:339–343.
18. **Bush LR, Romson JL, Ash JL, Lucchesi BR.** Effects of diltiazem on extent of ultimate myocardial injury resulting from temporary coronary artery occlusion in dogs. J Cardiovasc Pharmacol 1982;4:285–296.
19. **Lie JT, Pairolero PC, Holley KE, Titus JL.** Macroscopic enzymatic-mapping verification of large homogeneous, extensive myocardial infarctions of predictable size and location in dogs. J Thorac Cardiovasc Surg 1975;69:599–604.
20. **Hirzel HO, Nelson GR, Sonnenblick EH, Kirk ES.** Redistribution of collateral blood flow from necrotic to surviving myocardium following coronary occlusion in the dog. Circ Res 1976;39:214–222.
21. **Strauss HW, Harrison K, Langan JK, Lebowitz E, Pitt B.** Thallium-201 for myocardial imaging. Relation of thallium-201 to regional myocardial perfusion. Circulation 1975;51:641–645.
22. **Lucchesi BR, Burmeister WE, Lomas TE, Abrams GD.** Ischemic changes in the canine heart as affected by the dimethyl quaternary analog of propanolol, UM-272 (SC-27761). J Pharmacol Exp Ther 1975;199:310–328.
23. **Fishbein MC, Meerbaum S, Rit J, Lando U, Kanmalsuse K, Mercier JC, Corday E, Ganz W.** Early phase acute myocardial infarct size quantification: validation of the triphenyl tetrazolium chloride tissue enzyme staining technique. Am Heart J 1981;101:593–600.
24. **Reimer KA, Jennings RB.** The changing anatomic reference base of evolving myocardial infarction. Underestimation of myocardial collateral blood flow and overestimation of experimental anatomic infarct size due to tissue edema, hemorrhage and acute inflammation. Circulation 1979;60:866–876.